

The Emission Properties of Light Emitting Diodes using InGaN/AlGaIn/GaN Multiple Quantum Wells

A. E. Yunovich¹, V. E. Kudryashov¹, A. N. Turkin¹, A. Kovalev² and F. Manyakhin²

¹*M.V.Lomonosov Moscow State University,*

²*Moscow Institute of Steel and Alloys,*

(Received Sunday, June 21, 1998; accepted Friday, October 23, 1998)

Luminescence spectra of Light Emitting Diodes (LEDs) with Multiple Quantum Wells (MQWs) were studied at currents $J = 0.15 \mu\text{A} - 150 \text{ mA}$. A high quantum efficiency at low J is caused by a low probability of the tunnel current J (which is maximum at $J_m \approx 0.5-1.0 \text{ mA}$). $J(V)$ curves were measured in the range $J = 10^{-12}-10^{-1} \text{ A}$; at $J > 10^{-3} \text{ A}$ they may be approximated by a sum of four parts: $V = \phi_k + mkT \cdot [\ln(J/J_0) + (J/J_1)^{0.5}] + J \cdot R_s$. The part $V \sim (J/J_1)^{0.5}$ is the evidence of a double-injection into i-layers near MQWs. Their presence is confirmed by capacitance measurements. An overflow of carriers through the MQW causes a lower quantum efficiency at high J . A model of a 2D-density of states with exponential tails fits the spectra. The value of T in the active layer was estimated. A new band was detected at high J ; it can be caused by non-uniformity of In content in MQWs.

1 Introduction

Recombination mechanisms in InGaN/AlGaIn/GaN heterostructures are not fully understood in spite of the great progress in the development of GaN-based light-emitting diodes (LEDs). A model of radiative recombination in 2D-structures with band tails caused by potential fluctuations was successfully applied to luminescence spectra of LEDs with single quantum wells (SQW) [1] [2] [3] [4] [5] and radiative recombination by tunneling was detected at low currents [3] [4] [5] [6] [7] [8].

There is evidence of the fact that phase separation can take place during the growth of InGaN active thin layers (quantum wells). Clusters (quantum dots) with a higher In content may be formed [9]. But no attempts have been reported to describe the spontaneous emission spectra of LEDs using a model of recombination in such clusters.

It was interesting to study details of luminescence spectra of working LEDs recently developed with multiple quantum wells (MQW) [10] [11] and to compare their properties with those of LEDs with SQWs.

In this work samples of blue and green LEDs with MQW InGaIn/GaN active layers [10] [11] were studied

at a wide range of currents. A model of radiative recombination in 2D-structures with band tails is applied to describe the luminescence spectra. Charge and electric field distributions for LEDs with SQWs and MQWs are compared. The mechanisms of recombination in GaN-based MQWs are discussed.

2 Experimental

Blue and green LEDs based on $\text{In}_x\text{Ga}_{1-x}\text{N}/\text{Al}_y\text{Ga}_{1-y}/\text{GaN}$ heterostructures were studied [10] [11]. Structures were grown by MOCVD on sapphire substrates with an AlN buffer layer (30 nm) followed by a base n-GaN: Si layer (4–5 μm). An $\text{In}_x\text{Ga}_{1-x}\text{N}/\text{GaN}$ MQW structure was grown on the base. The number of periods in the MQW varied; samples with 5 periods were chosen for the study; the thickness of each period was less than 8 nm. The upper layer of $\text{Al}_y\text{Ga}_{1-y}\text{N}$ (50 nm) and a cap layer GaN (0.5 μm) were Mg-doped. The indium content in the wells varied, with $x = 0.2-0.4$. This value determined the spectral range of the luminescence, blue ($x \approx 0.2$) or green ($x \approx 0.4$). In order to look at details of the spectra, a wide interval of forward currents J was used (0.1 $\mu\text{A}-200 \text{ mA}$); pulsed measurements were used at $J > 10 \text{ mA}$ (50 Hz, 5 μs).

3 Experimental results.

3.1 Luminescence spectra of LEDs

Spectra of 10 blue and 10 green LEDs were studied. The room temperature spectral maxima of the blue LEDs at $J = 10$ mA were $\hbar\omega_{\max} = 2.64\text{--}2.67$ eV, ($\lambda_{\max} = 465\text{--}467$ nm), and the spectral width was $\Delta(\hbar\omega)_{1/2} = 0.21$ eV ($\Delta(\lambda)_{1/2} = 36\text{--}37$ nm). The maxima for green LEDs were $\hbar\omega_{\max} = 2.35\text{--}2.37$ eV, ($\lambda_{\max} = 465\text{--}467$ nm), spectral width $\Delta(\hbar\omega)_{1/2} = 0.21$ eV ($\Delta(\lambda)_{1/2} = 36\text{--}37$ nm).

Spectra of blue and green LEDs at currents in the range $J = 10^{-7}\text{--}10^{-1}$ A are shown in Figure 1 and Figure 2. The lower currents at which spectra are shown is ≈ 0.15 μ A for blue and ≈ 0.5 mA for green LEDs. We have not seen room-temperature spectra of GaN-based LEDs at such low currents in the literature. The maxima of the spectra of the blue LEDs move with the current in the range $\hbar\omega_{\max} = 2.57\text{--}2.67$ eV, in contrast to blue SQW LEDs in which the blue maximum does not shift with the current [3] [4] [5]. There is no additional band in the yellow-green region moving with the voltage at low currents. Such a band was described as a tunnel band in blue SQW LEDs [5] [6] [7]. The maxima of the spectra of the green LEDs move in the range $\hbar\omega_{\max} = 2.2\text{--}2.45$ eV, a wider range than in green SQW LEDs [3] [4] [5].

The low-energy sides of the spectra have an exponential form $I \sim \exp(\hbar\omega/E_0)$. The parameter E_0 had the value $E_0 \approx 50\text{--}60$ meV, and changed only slightly with the current, as occurred in the spectra of SQW LEDs [3] [4] [5]. The high-energy sides also have an exponential form, $I \sim \exp(-\hbar\omega/E_1)$. The value of E_1 was about 40–50 meV, not equal to kT . A new band could be detected (as shoulders, $\hbar\omega = 2.7\text{--}2.8$ eV) on the high-energy tails of the spectra of green LEDs at higher currents (see Figure 2). The value of E_1 in the high-energy tails of the spectra of blue LEDs was proportional to T in the range $T = 220\text{--}290$ K, $E_1 = m \cdot kT$, $m = 1.3\text{--}1.6$.

3.2 Spectral shift with current and voltage

Spectra of blue LEDs at higher currents are shown in Figure 3 ($J = 20\text{--}150$ mA). The maxima of the spectra at constant (dc) current move to lower energies for $J > 40$ mA (see Figure 3a). The parameter E_1 in the high-energy exponential tails grew with this shift. The maxima of the spectra at pulsed currents (50 Hz, 5 μ s) moved to higher energies; the parameter E_1 remained unchanged (see Figure 3b). Heating of LEDs at high dc currents may explain these facts. A dependence of $\hbar\omega_{\max}$ of the energy eV (V-voltage) is shown in Figure 4. In a comparatively wide range of voltage this function is linear, but the slope of the line is $\ll 1$, (in contrast

with the tunnel band reported in [3] [4] [5] [6]). Filling of the tail states in the active layer causes this shift.

3.3 Current-voltage characteristics

Current-voltage characteristics $J(V)$ of blue and green LEDs are shown in Figure 5. There is an exponential part at low currents, $J < 10^{-7}$ A at 300 K, a steep exponential growth in the range $V = 2.3\text{--}2.7$ V, a linear part at higher currents, $J > 20$ mA. Low currents can be understood as a tunnel component; tunnel currents in these LEDs play some role at J 3-4 orders of magnitude lower than that for SQW-based LEDs [3] [4] [5] [6] [7]; $J(V)$ curves of SQW-based LEDs are shown in Figure 5 for comparison. The difference can be explained as a consequence of a wider active layer of MQW structures.

A good approximation of the $J(V)$ curves for MQW LEDs was made when not only a series resistance R_s at the linear part at higher J was taken into account, but also the quadratic part: $J \sim (V-V_1)^2$. The fit of the curve $J(V)$ at $J > 0.1$ mA by the equation:

$$V = \phi_k + E_j [\ln(J/J_0) + (J/J_1)^{0.5}] + J \cdot R_s, \quad (1)$$

is shown in Figure 5. The fitting parameters are ϕ_k (contact potential), E_j ($E_j = c \cdot kT$, $c = 1\text{--}2$), J_0 (saturation current), and J_1 , R_s . One part $\sim (J/J_1)^{0.5}$ is sufficient between an exponential (injection) and a linear parts, in the usual working current range $J = 2\text{--}30$ mA..

3.4 Quantum efficiency

Dependencies of the integrated intensity $\Phi(J)$ and external quantum efficiency $\eta_e(J) = e\Phi/J$ versus J are shown in Figure 6. Measurements of η_e were done by a method described in [12]. The efficiency $\eta_e(J)$ has a maximum at low currents $J \approx 0.5\text{--}1.0$ mA, at the start of the steep exponential growth of $J(V)$. The value of η_e goes down logarithmically with J at high currents (linearly with V).

3.5 Distribution of charged centers.

The distributions of charged centers in p- regions of MQW and SQW InGaN/AlGaIn/GaN p-n- heterostructures are shown in Figure 7 (see the measurement method in [13]). The MQW LEDs space charge is wider than that of SQW LEDs [3] [4] [5] [6]; in both cases the width for green LEDs is wider than for blue ones. This fact corresponds to a low probability of tunneling in the MQW LEDs.

It seems that high Mg-doping of p-AlGaIn and GaIn layers is more difficult for higher In concentration in InGaIn active layers.

4 Discussion

4.1 Spectral fit by the model of 2D-density of states with low-energy tails.

We describe the spectra with a model previously applied for fitting the spectra of SQW LEDs [1] [2] [3] [6]. The model implies that an effective radiative recombination takes place when carriers of both signs are injected into the active layer at voltages on the layer $U < V$. The value of U is close to ϕ_k . Optical transitions at $\hbar\omega$ are going between states $E_{(c)}$ and $E_{(v)}$ in the tails of the 2D-structure caused by potential fluctuations. A model 2D joint density of states is

$$N^{2D}(\hbar\omega - E_g^{\text{eff}}) = [1 + \exp(-(\hbar\omega - E_g^{\text{eff}})/E_0)]^{-1}; \quad (2)$$

an effective energy gap E_g^{eff} is $E_g^{\text{eff}} = E_c^* - E_v^*$. The parameter E_0 is determined by potential fluctuations. A discussion of possible sources of these fluctuations (well and barrier inhomogeneities, fields due to impurities, or piezoelectric effects) will be published elsewhere.

The spectral intensity $I(\hbar\omega)$ is proportional to the Fermi-functions of electrons and holes with quasi-Fermi levels F_n, F_p as parameters (details in Ref. [5]):

$$I(\hbar\omega) \sim N^{2D}(\hbar\omega - E_g^{\text{eff}}) f_c(\hbar\omega, m, kT, F_n) (1 - f_v(\hbar\omega, 1-m, kT, F_p)); \quad (3)$$

$$F_n - F_p = eU; \quad \hbar\omega = E_{(c)} - E_{(v)}; \quad 1 < m < 2.$$

Examples of the fit are shown in Figure 1 and Figure 2; parameters of the fit are summarized in Table 1. It is possible to describe a change of $\hbar\omega_{\text{max}}$ in a certain range of J by changes of the parameter F_n – the parameters E_g^{eff} , E_0 and $E_1 = m \cdot kT$ may be unchanged. This is evidence of the fact that the mechanism of recombination in the 2D tail-states is not changed.

4.2 Parameters of the approximation

This description is valid only in some range of J . The parameter $E_1 = m \cdot kT$ changes at higher J . This is caused first of all by heating at $J > 10$ mA. Curves of approximation are shown in Figures 3a, 3b. It is possible to describe shifts of pulse spectra without changing the parameter E_1 , and shifts of the dc spectra - without changing the parameter m , supposing a change of temperature T . The low energy shift of spectral maxima at higher J corresponds to the empirical equation of Varshni:

$$E_g^{\text{eff}}(T) = E(0) - \alpha T^2 / (\beta + T). \quad (4)$$

The parameters in this equation are $E(0) = 3.07$ eV; $\alpha = 12.8 \cdot 10^{-4}$ eV/K; $\beta = 1190$ K (see [14]).

4.3 Possible origin of the new spectral band

The short wavelength tail changes not only by heating, but also with the current. It depends also on the new spectral band that is clearly seen in the logarithmic scale on the spectra (see Figure 2). We suppose that this band is caused by large-scale inhomogeneities - separation of phases with different content of indium in $\text{In}_x\text{Ga}_{1-x}\text{N}$. Models of recombination either in the band tails or quantum dots were examined as an alternative in the discussion at the Tokushima Conference [10]. It seems that our results confirm that both possibilities are realized. The proof of our supposition may be obtained by studying the luminescence of MQWs with microstructures revealed by electron microscopy and SIMS.

4.4 Maximum quantum efficiency

The problem of the maximum η_e versus J is a very important one. It is connected to the number of QWs and to the properties of p-AlGaIn layers made by various technologies.

This maximum can be understood as follows. Non-radiative channels of recombination (for example, tunnel recombination) take place at low J . Electrons are filling the active MQW layer by injection. This is the region of maximum η_e . At higher J electrons overflow the active layer and are pulled by an electric field into the i-layer and p-AlGaIn (see an analogous model in [15]). The quadratic part of the $J(V)$ and the linear dependence $\eta_e(V)$ show the role of electric field and of a drift component of the current.

5 Conclusions

1. Luminescence spectra of LEDs based on InGaIn/AlGaIn/GaN heterostructures were studied in a wide range of currents, down to $J = 10^{-7}$ A at room temperature. Filling the tail states in MQWs causes shifts of the spectral maxima with the voltage.
2. The model of recombination in a 2D-structure with exponential band tails describes the spectra with good accuracy. A new spectral band was detected; it is supposed that this band can be caused by phases of higher indium concentrations in InGaIn QWs.
3. The tunnel component of the current is 3-4 orders of magnitude lower than in analogous SQW LEDs. The LEDs have a current component described by a model of double injection of carriers into the i-layers adjacent to the active MQW layer.
4. The quantum efficiency has a maximum depending on the current. Overflow of electrons through the active layer can cause lower quantum efficiency at higher cur-

rents; an electric field is pulling the carriers into compensated i-layers.

ACKNOWLEDGMENTS

Authors are grateful to Dr. M.Koike (Toyoda Gosei Co. Ltd.) for sending LEDs to Moscow University. Two authors (A.E.Y. and V.E.K.) thank International Soros Science Education Program for a financial support.

REFERENCES

- [1] S. Nakamura, M. Senoh, N. Iwasa, S. Nagahama, *Jpn. J. Appl. Phys.* **34**, L797-L799 (1995).
- [2] S. Nakamura, M. Senoh, N. Iwasa, S. Nagahama, T. Yamada, T. Mukai, *Jpn. J. Appl. Phys.* **34**, L1332-L1335 (1995).
- [3] K. G. Zolina, V. E. Kudryashov, A. N. Turkin, A. E. Yunovich, Shuji Nakamura, *MRS Internet J. Nitride Semicond. Res.* **1**, 11 (1996).
- [4] K.G.Zolina, V.E.Kudryashov, A.N.Turkin, A.E.Yunovich, S.Nakamura, "Spectra of Superbright Blue and Green InGaN/AlGaIn/GaN Light-Emitting diodes", *Refer. Rep. of the Journal of European Ceramic Soc.* **17**, 2033 (1997)
- [5] K. G. Zolina, V. E. Kudryashov, A. N. Turkin, A. E. Yunovich, *Semiconductors* **31**, 901 (1997).
- [6] A. E. Yunovich, A. N. Kovalev, V. E. Kudryashov, F. I. Manyachin, A. N. Turkin, K. G. Zolina, *Mater. Res. Soc. Symp. Proc.* **449**, 1167 (1997).
- [7] V. E. Kudryashov, K. G. Zolina, A. N. Turkin, A. E. Yunovich, A. N. Kovalev, F. I. Manyachin, *Semiconductors* **31**, 1123 (1997).
- [8] A. E. Yunovich, V. E. Kudryashov, A. N. Turkin, K. G. Zolina, A. N. Kovalev, F. I. Manyachin, *Electrochem. Soc. Proc.* **97-34**, 83 (1998).
- [9] F. Manyachin, A. Kovalev, V. E. Kudryashov, A. N. Turkin, A. E. Yunovich, *MRS Internet J. Nitride Semicond. Res.* **2**, 11 (1997).
- [10] 2nd Int. Conference on Nitride Semiconductors, Tokushima, Japan, (1997)
- [11] H. Sakai, T. Koide, H. Suzuki, M. Yamaguchi, S. Yamasaki, M. Koike, H. Amano, I. Akasaki, *Jpn. J. Appl. Phys.* **34**, L1429-L1431 (1995).
- [12] A. N. Turkin, A. E. Yunovich, *Tech. Phys. Lett.* **22**, 989 (1996).
- [13] F.I.Manyachin, A.N.Kovalev, V.E.Kudryashov, A.N.Turkin, A.E.Yunovich, *Semiconductors*, **32** (10), (1998, to be published)
- [14] Alexey V. Dmitriev, Alexander L. Oruzhenikov, *MRS Internet J. Nitride Semicond. Res.* **1**, 46 (1996).
- [15] Kay Domen, Reiko Soejima, Akito Kuramata, Toshiyuki Tanahashi, *MRS Internet J. Nitride Semicond. Res.* **3**, 2 (1998).

FIGURES

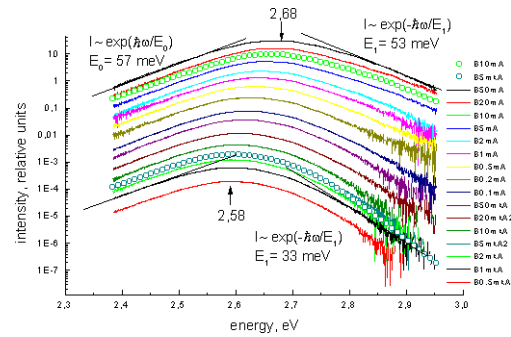


Figure 1. Luminescence spectra of a blue LED N17 (room temperature) at different currents, numbers - J, mA; points - approximations by equation (2).

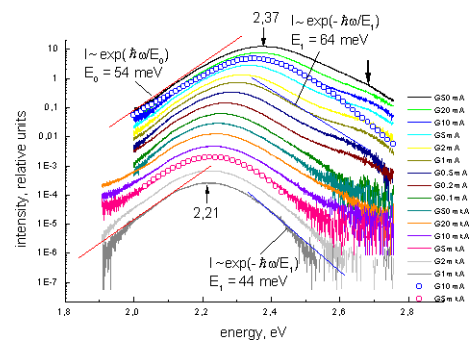


Figure 2. Luminescence spectra of a green diode N18 (room temperature) at different currents, numbers - current J; points - approximations by equation (2).

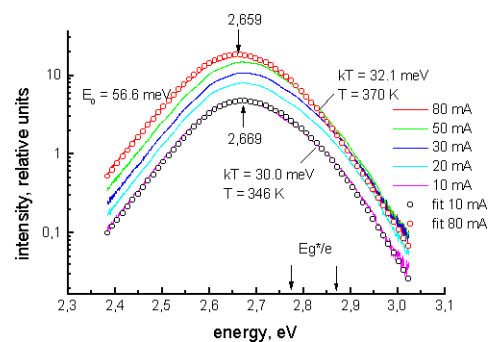


Figure 3a. Spectra of a blue LED N13 at high currents in dc conditions; points - approximation by equation (2).

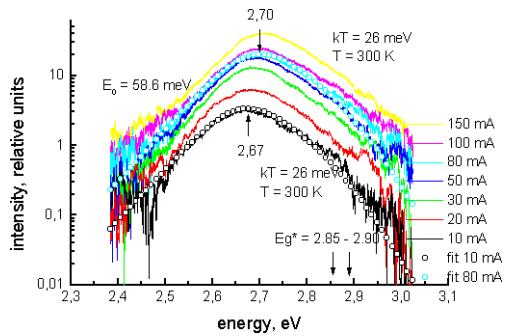


Figure 3b. Spectra of a blue LED N13 at high currents in pulse conditions (50 Hz, 5 μ s); points - approximation by equation (2).

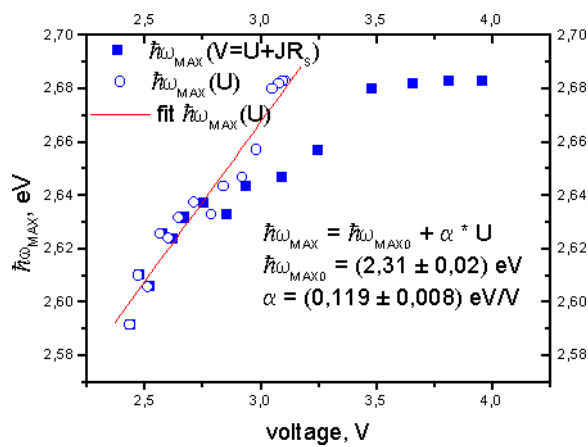


Figure 4a. Dependence of spectral maxima of a blue LED B17 versus voltage in dc conditions.

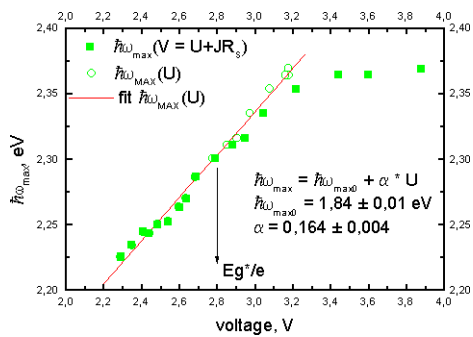


Figure 4b. Dependence of spectral maxima of a green LED G18 versus voltage in dc conditions.

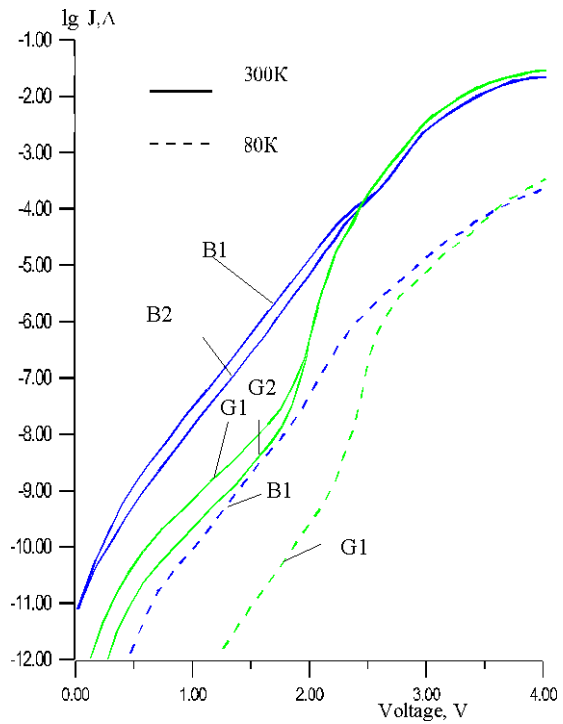


Figure 5. Current-voltage characteristics of blue (B1, B2) and green (G1, G2) LEDs with single (B1, G1) and multiple (B2, G2) QW at room temperature (solid curves) and at 80 K (dashed).

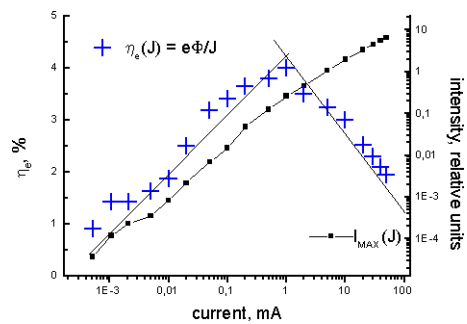


Figure 6a. Dependence of integrated intensity and quantum efficiency for a blue B17 diode on the current.

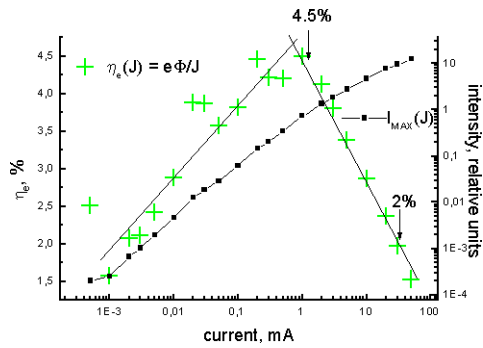


Figure 6b. Dependence of integrated intensity and quantum efficiency for a green G18 diode on the current.

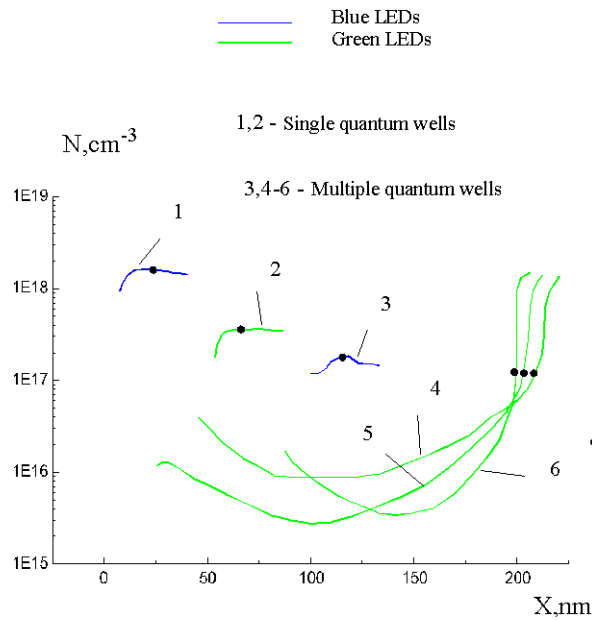


Figure 7. Distributions of charged centers in p-regions of p-n heterojunctions; points - values of N_A^- at $V = 0$; beginning of abscissa is at the n-interface. Blue (1,3) and green (2,4-6) LEDs with single (1,2) and multiple (3-6) quantum wells.

TABLES

Table 1. Fitting parameters for approximating blue LED spectra

J , mA	U , V	$h\nu_{max}$, eV	E_0 , meV	m	ΔF_V , eV	E_g^{eff} , eV
10	3,023	2,664	57,61	1,582	-0,149	2,860
1	2,773	2,628	57,61	1,582	-0,155	2,791
0,1	2,597	2,608	55,18	1,580	-0,169	2,842
0,01	2,510	2,585	52,00	1,720	-0,176	2,826